

T-Shaped Z-Source Inverter

Sheeja P.Kumar¹, P.Shailaja²

*Department of Electrical and Electronics Engineering, Teegala Krishna Reddy Engineering College
JNTU, Hyderabad, India*

Abstract—This paper extends the impedance source (Z-source) inverters concept to the T-Shaped Z-source inverters in PV solar panels. The availability, utility and cost is implemented best output of the solar panels. T-Shaped Z-Source consists of one transformer and a capacitor connected such that a T-Shape is formed. Hence the name is T-Shaped. The T-Shaped Z-Source inverter is divided into two parts, the first part is step up or step down dc to dc voltage using T-Shaped Z-Source and the inverter converts dc to ac. The voltage fed T-Shaped z source inverter is used to convert solar step up voltage DC to AC voltage. In this paper sinusoidal pulse width modulation is used to control the switches. Thus the output generated is sine wave. While maintaining the main features of the previously presented Z-source network, the new networks exhibit some unique advantages, such as the cost is reduced increasing the availability as d.c is taken from solar panels. Also the increased voltage gain and reduced voltage stress in the voltage-fed trans-ZSI. The simulation results for the voltage fed PV system are presented for analysis.

Keywords— Photo Voltaic, DC-DC conversion using T-Shaped Z-Source, DC-ac Conversion using inverter

I. INTRODUCTION

As the energy resources and their utilization will be a prominent issue of this century, the problems of natural resource depletion, environmental impacts, and the rising demand for new energy resources have been discussed fervently in recent years. Several forms of renewable zero pollution energy resources, including wind, solar, bio, geothermal and so forth, have gained more prominence and are being researched by many scientists and engineers [1-2]. Solar cell installations involve the use of multiple solar panels or modules, which can be connected in series or in parallel to provide the desired voltage level to the inverter. The cascaded H-bridge multilevel inverter topology requires a separate DC source for each H-bridge so that high power and/or high voltage that can result from the combination of the multiple modules in a multilevel inverter would favour this topology [3-7]. To maximize the energy harvested from each string, a maximum power point tracking (MPPT) strategy is needed. The task of finding the optimum operation point might increase the complexity and component count as the number of isolated DC sources increase. The approach chosen to deal with the number of input sources was to monitor AC output power parameters instead of DC input measurements. Traditional voltage-source inverters (VSIs) and current source

inverters (CSIs) have similar limitations and problems. For VSIs: 1) The obtainable ac output voltage cannot exceed the dc source voltage. So a dc-dc boost converter is needed in the applications, for instance, with limited available dc voltage or with the demand of higher output voltage. 2) Dead time is required to prevent the shoot-through of the upper and lower switching devices of each phase leg. However, it induces waveform distortion. For CSIs: 1) Their output voltage cannot be lower than the dc input voltage. 2) Overlap time between phase legs is required to avoid the open circuit of all the upper switching devices or all the lower devices. The Z-source inverter (ZSI) [1], as well as the derived quasi Z-source inverters (qZSI) [2, 3], can overcome the above problems. They advantageously utilize the shoot-through of the inverter bridge to boost voltage in the VSIs (or open circuit in the CSIs to buck voltage). Thus, buck-boost functionality is achieved with a single stage power conversion. They also increase the immunity of the inverters to the EMI noise [4], which may cause misgating and shoot-through (or open-circuit) to destroy the conventional VSIs and CSIs. The voltage-fed Z-source inverter can have theoretically infinite voltage boost gain. However, the higher the voltage boost gain is, the smaller modulation index has to be used. In applications such as grid-connected photovoltaic (PV) generation and fuel cell power conversion, a low voltage dc source has to be boosted to a desirable ac output voltage. A small modulation index results in a high voltage stress imposed on the inverter bridge. Several pulse width modulation (PWM) methods [5, 6] have been developed with the attempt of obtaining as much voltage gain as possible and thus limiting the voltage stress across the switching devices. The maximum boost control [5] achieves the maximum voltage gain through turning all the zero states in the traditional VSIs to shoot-through zero states. Nevertheless, it brings in low frequency ripples associated with the ac side fundamental frequency. So the constant boost control [6] has been proposed to eliminate those ripples and thus reduce the L and C requirement in the Z-source network, with slightly less voltage gain, compared to the maximum boost control. These PWM methods still have limits to further extend the voltage gain without sacrificing the device cost. Recently, some modified impedance source networks were proposed in [7-10] for the sake of increasing the output voltage gain. Among them, a T-source inverter [7] has the possibility of increasing voltage gain with the minimum component count. As will be discussed in the next section, it can be grouped into a general class of transformer based Z-source inverters called T-Shaped-ZSIs presented in this paper,

which employ two transformer windings in the impedance network. The voltage-fed Z source/quasi Z-source inverters cannot have bidirectional operation unless replacing the diode with a bidirectional conducting, unidirectional blocking switch [11]. Neither can the traditional current-fed inverters ([12-14]) do unless they are fed by a phase-controlled rectifier in front that can change the dc link voltage polarity. Interestingly, the current-fed Z-source/quasi Z-source inverters [2, 15, 16] can have voltage buck-boost and bidirectional power flow only with a diode in the impedance network. With the newly developed reverse blocking IGBTs [17], this single stage power converter becomes a promising topology. Yet, their dc-ac voltage gain cannot exceed two in the boost mode operation. In other words, the dc input voltage cannot be lower than half of the peak output line-to-line voltage. Hence, this paper further proposes two current-fed T Shaped Z-source inverters that are capable of reaching wider voltage boost range and bidirectional power flow with a single diode. As a result, a wider output voltage range can be obtained, which is [8].essential to some applications such as HEV/EV motor drives. The T-Shaped Z-source inverters can be derived from the voltage-/current-fed quasi Z-source inverters or the voltage- /current-fed Z-source inverters. The T-Shaped Z-source-inverters inherit their unique features, and they can be controlled using the PWM methods applicable to the Z-source inverters. This paper will begin with the derivation of two voltage-fed T-Shaped Z-source-inverters from one of the quasi Z-source inverters. simulation results will demonstrate their new properties different from the Zsource/ quasi Z-source inverters.

II. THE VOLTAGE-FED TSHAPED-Z-SOURCE INVERTERS

Fig.1. shows the voltage-fed T-Shaped Z-source inverter consists of three main parts: Solar panel (MPPT), a d.c link circuit and an inverter bridge. The d.c link circuit is implemented by the Z-source network (L1, L2, and C1). In the voltage fed T-Shaped Z-Source inverter, d.c link is used to boost the voltage and the boosted voltage is converted to a.c voltage by means of an inverter bridge.

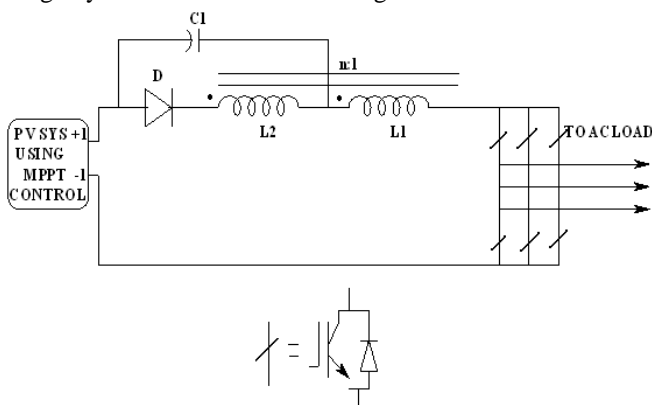


Fig.1 voltage fed T-Shaped z source inverter

In the voltage fed T-Shaped Z Source inverter single transformer with a capacitor is connected such that it forms T-

Shape. The linear transformer behaves more or less like an inductor which is magnetically coupled. When the two inductors are coupled as shown in Fig.2, the voltage across the inductor L1 is reflected to the inductor L2. Also, the voltage across L2 can be made proportional to the voltage across L1 by changing the turnsratio $n2 / n1$. The T-Shaped quasi Z source inverter has an extra shoot-through zero state besides the six active states and two traditional zero states [18]. For the purpose of analysing the characteristics of the T-Shaped Z-source inverters, this paper will focus on the two general continuous current modes as in the Zsource inverter: the shoot-through zero state and the non-shoot-through states [1, 19].

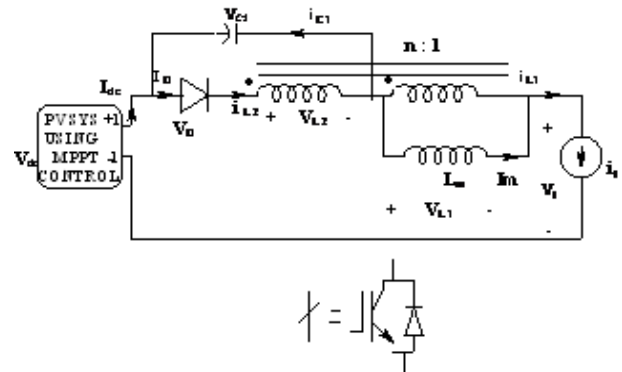


Fig.2 Voltage-fed T-Shaped quasi-Z -source inverter

In the shoot-through zero state, the inverter is equivalent to a short circuit as shown in Fig. 3(a). The diode is reversed biased. Note that the symbol Dsh is used here for shoot-through duty ratio in voltage-fed Zsource inverters. During the shoot-through zero state for an interval of $DshT$, the voltages across L1 and L2 are:

$$V_{L1} = V_{dc} + V_{C1} \quad (1)$$

$$V_{L2} = \frac{n2}{n1} V_{L1} \quad (2)$$

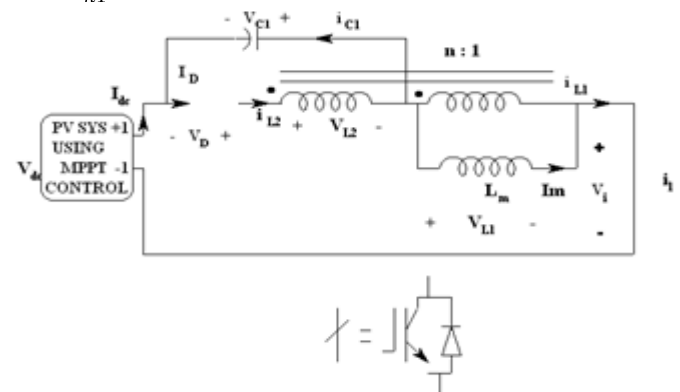


Fig.3 (a) The equivalent circuits of the voltage-fed T-Shaped qZSI viewed from the dc link, shoot-through states

In the non-shoot-through states for an interval of $(1 - Dsh) T$, the inverter bridge can be modelled as an equivalent current source as shown in Fig. 3(b). The non-shoot-through states

include the six active states and two traditional zerostates. For the non-shoot through zero state, the inverter is equivalent to an open circuit. During the non-shoot through zero state the voltages across L1 and L2 are:

$$V_{L2} = -V_{C1} \tag{3}$$

$$V_{L1} = \frac{n1}{n2} V_{L2} = -\frac{n1}{n2} V_{C1} \tag{4}$$

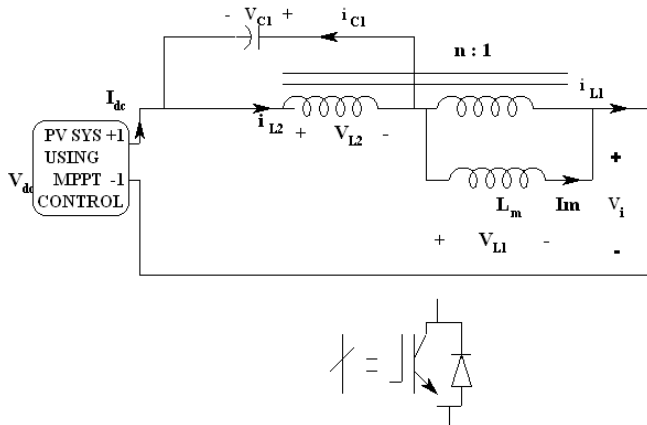


Fig. 3(b) the equivalent circuits of the voltage-fed T-Shaped qZSI viewed from the dc link(b) Non-shoot-through states

The average voltage of both inductors should be zero over one switching period in the steady state. Thus, the voltage across L1 is:

$$V_{L1} = \frac{(V_{dc} + V_{C1})D_{sh}T + (-\frac{n1}{n2}V_{C1})(1 - D_{sh})T}{T} = 0 \tag{5}$$

From the above equation, the capacitor voltage can be calculated as:

$$V_{C1} = \frac{nD_{sh}}{1 - (1+n)D_{sh}} V_{dc} \tag{6}$$

When $n = n2/n1 > 0$

From (4) and (6), the dc link voltage across the bridge in the non-shoot-through states can be boosted to:

$$\hat{V}_i = \frac{1}{1 - (1+n)D_{sh}} V_{dc} = BV_{dc} \tag{7}$$

Where the boost factor is:

$$B = \frac{1}{1 - (1+n)D_{sh}} \tag{8}$$

The peak value of the phase voltage from the inverter output:

$$\hat{V}_{ph} = M \cdot \hat{V}_i / 2 = M \cdot B \cdot V_{dc} / 2 \tag{9}$$

Where M is the modulation index. When the constant boost control [6] is used, the voltage gain (MB) as defined in [5] is:

$$G = MB = \frac{M}{1 - (1+n)(1 - \frac{\sqrt{3}}{2}M)} \tag{10}$$

It can be seen that if the turns ratio is 1, the inverter dc link voltage boost gain is the same with that of the original Z source/ quasi Z-source inverters, but one capacitor is saved in the new T-Shaped Z-source network. If the turns-ratio is over 1, the inverter dc link voltage boost gain can be higher given the same modulation index, M . In other words, it needs a smaller shoot-through duty ratio D_{sh} (accordingly a larger modulation index M) to produce the same ac output voltage than the Z source/ quasi Z-source inverters do. The voltage gain (MB) versus the modulation index for the voltage-fed T-Shaped quasi-Z source inverter (with a turns ratio $n=2$) is compared in Fig. 4 with that for the Z-source/quasi Z-source inverters, using the constant boost control.

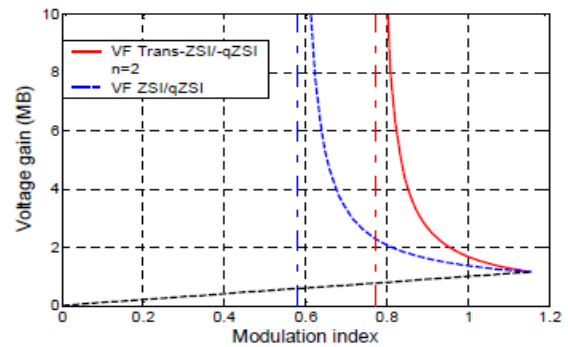


Fig. 4 Voltage gain (MB) versus modulation index of the voltage-fed T-Shaped ZSI-qZSI ($n=2$) and ZSI/qZSI.

The voltage stress, V_s across the switching devices can be assessed by comparing its peak dc link voltage against the minimum dc voltage (GV_{dc}) [6] needed for the traditional VSI to produce the same ac output voltage at $M=1$. The ratio represents extra cost that the voltage-fed trans-quasi-Z-source inverter and Z-source/quasi Z-source inverters have to pay for the voltage boost in association with the higher voltage stress. In Fig. 5, the voltage-fed trans-Z-source inverter has less voltage stress across the inverter bridge for the same dc-ac output voltage gain. Hence, this circuit is beneficial to applications, in which a high voltage gain is required.

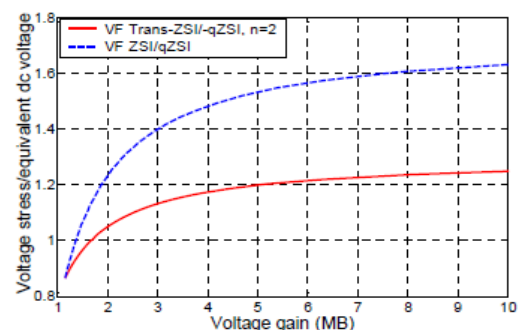


Fig. 5 Active switch voltage stress of voltage-fed T-Shaped ZSI-qZSI ($n=2$) and ZSI/qZSI.

III. MPPT CONTROL FOR PV SYSTEM

A solar cell is comprised of a P-N junction semiconductor that produces currents via the photovoltaic effect. PV arrays are constructed by placing numerous solar cells connected in series and in parallel. A PV cell is a diode of a large-area forward bias with a photovoltage and the equivalent circuit is shown in Figure 6.

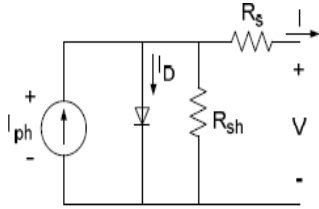


Fig.6 PV Cell equivalent circuit

The current-voltage characteristic of a solar cell is derived as follows:

$$I = I_{ph} - I_D \quad (11)$$

$$I = I_{ph} - I_0 \left[\exp\left(\frac{q(V + I R_s)}{A T K_B}\right) - 1 \right] - \frac{(V + I R_s)}{R_{sh}} \quad (12)$$

Where

I_{ph} = photocurrent,

I_D = diode current,

I_0 = saturation current,

A = ideal factor,

q = electronic charge 1.6×10^{-19} ,

k_B = Boltzmann's gas constant (1.38×10^{-23}),

T = cell temperature,

R_s = series resistance,

R_{sh} = shunt resistance,

I = cell current,

V = cell voltage

Typically, the shunt resistance (R_{sh}) is very large and the series resistance (R_s) is very small. Therefore, it is common to neglect these resistances in order to simplify the solar cell model. The resultant ideal voltage-current characteristic of a photovoltaic cell is given by and illustrated by Figure 7.

$$I = I_{ph} - I_0 \left[\exp\left(\frac{qV}{kT}\right) - 1 \right] \quad (13)$$

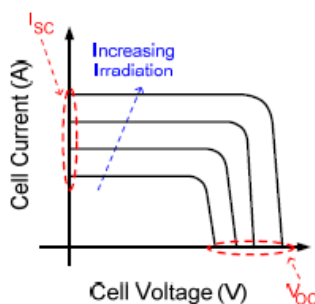


Fig 7: PV cell voltage-current characteristic

The typical output power characteristics of a PV array under various degrees of irradiation is illustrated by Figure 8. It can be observed in Figure 7 that there is a particular optimal voltage for each irradiation level that corresponds to maximum output power. Therefore by adjusting the output current (or voltage) of the PV array, maximum power from the array can be drawn.

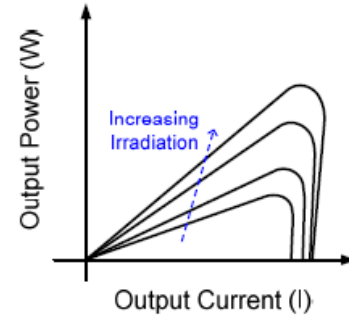


Fig8 PV cell power characteristics

Due to the similarities of the shape of the wind and PV array power curves, a similar maximum power point tracking scheme known as the hill climb search (HCS) strategy is often applied to these energy sources to extract maximum power. The HCS strategy perturbs the operating point of the system and observes the output. If the direction of the perturbation (e.g. an increase or decrease in the output voltage of a PV array) results in a positive change in the output power, then the control algorithm will continue in the direction of the previous perturbation. Conversely, if a negative change in the output power is observed, then the control algorithm will reverse the direction of the previous perturbation step. In the case that the change in power is close to zero (within a specified range) then the algorithm will invoke no changes to the system operating point since it corresponds to the maximum power point (the peak of the power curves). The MPPT scheme employed in this paper is a version of the HCS

IV. SINUSOIDAL PULSE WIDTH MODULATION

In the most straightforward implementation, generation of the desired output voltage is achieved by comparing the desired reference waveform (modulating signal) with a high frequency triangular 'carrier' wave as depicted schematically in Fig.9. Depending on whether the signal voltage is larger or smaller than the carrier waveform, either the positive or negative dc bus voltage is applied at the output. Note that over the period of one triangle wave, the average voltage applied to the load is proportional to the amplitude of the signal (assumed constant) during this period. The resulting chopped square waveform contains a replica of the desired waveform in its low frequency components, with the higher frequency components being at frequencies of an order close to the carrier frequency. Notice that the root mean square value of the ac voltage waveform is still equal to the dc bus voltage, and hence the total harmonic distortion is not affected by the PWM process. The harmonic components are merely shifted into the higher

frequency range and are automatically filtered due to inductances in the ac system.

When the modulating signal is a sinusoid of amplitude A_m , and the amplitude of the triangular carrier is A_c , the ratio $m=A_m/A_c$ is known as the modulation index. Note that controlling the modulation index therefore controls the amplitude of the applied output voltage. With a sufficiently high carrier frequency, the high frequency components do not propagate significantly in the ac network (or load) due to the presence of the inductive elements. However, a higher carrier frequency does result in a larger number of switchings per cycle and hence in an increased power loss. Typically switching frequencies in the 2-15 kHz range are considered adequate for power systems applications. Also in three-phase systems it is advisable to use $f_c/f_m=3k$, so that all three waveforms are symmetric.

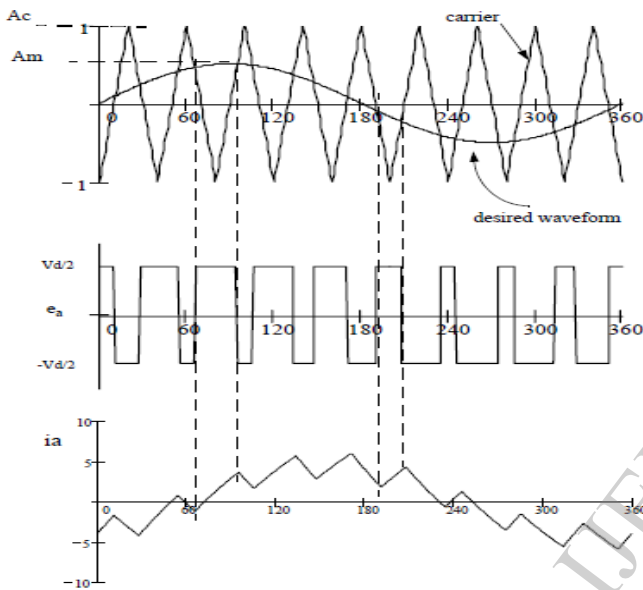


Fig 9: Principal of Pulse Width Modulation

Note that the process works well for .For, there are periods of the triangle wave in which there is no intersection of the carrier and the signal as in Fig.9. However, a certain amount of this “over modulation” is often allowed in the interest of obtaining a larger ac voltage magnitude even though the spectral content of the voltage is rendered somewhat poorer. Note that with an odd ratio for f_c/f_m , the waveform is anti-symmetric over a 360 degree cycle. With an even number, there are harmonics of even order, but in particular also a small dc component. Hence an even number is not recommended for single phase inverters, particularly for small ratios of f_c/f_m .

V.SIMULATION RESULTS

In this section the simulation results showed in MATLAB .her the Pv solar panels as input supply taking input supply as 100V .the MPPT controller is employed to get accurate solar power to the load .A voltage fed trans z source inverter is placed in the circuit with the inductor value of 1mH &

capacitor value of 10micro farads. An isolated transformer placed to perform buck –boost operation of z source inverter In above figure shown the input voltage trms z source inverter in that the irradiance of solar panel is 100V but according to the mppt controller algorithm the voltage is increased to 140V.In Fig 13 capacitor voltage of quasi voltage fed trans z source inverter is shown the capacitor will whatever voltage applied to the transformer and perform the buck –boost operation.

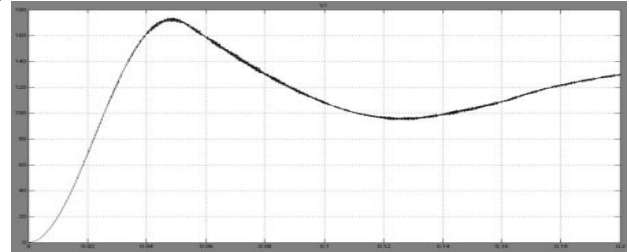


Fig 13 Quasi voltage fed trans z source inverter capacitor voltage

The pulse are produced to the inverter by using sinusoidal pulse width modulation in sinusoidal pulse width modulation the reference signal compares the carrier signal produces switching pulses. The switching frequency of inverter is 2000Hz. Modulation index , modulation frequency given as 0.8 & 50Hz.because of sinusoidal pulse width modulation the harmonic distortion will be very less compare to traditional modulation techniques. Inverter output voltage & currents is shown in fig15 & 16 the output voltage is varied to 140 volts & current is 7 amps getting as inverter output voltage.

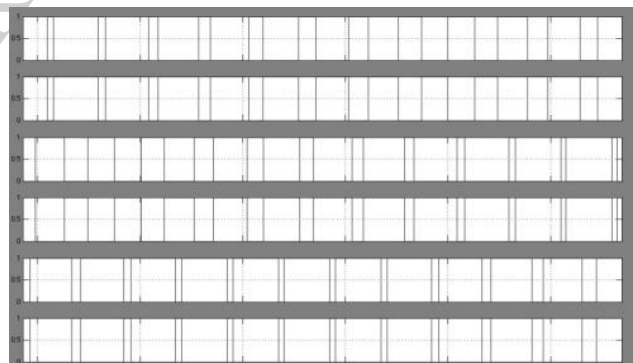


Fig10 Pulses produced to inverter

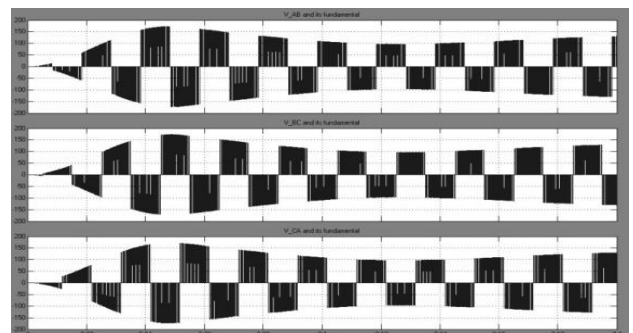


Fig 11 Inverter Output voltage

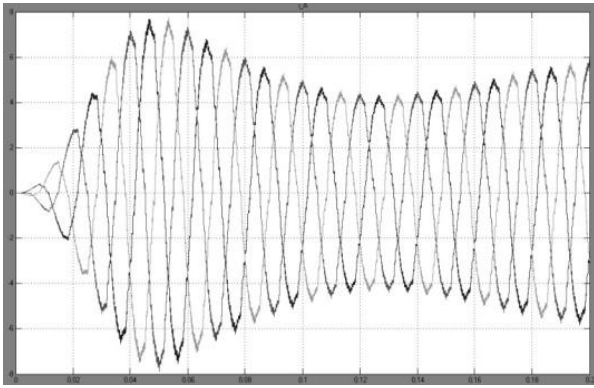


Fig 16 Inverter output currents

VI CONCLUSION

A class of trans-Z-source inverters has been presented for voltage-fed dc-ac inversion systems in PV system. When the turns-ratio of the two windings is over 1, the voltage-fed trans-Z-source inverter can obtain a higher boost gain with the same shoot-through duty ratio and modulation index, compared with the original Z-source inverter. With new unique features, they can broaden applications of the Z-source inverters. For instance, the voltage-fed trans-Z-source inverters provide a promising potential in the applications with very low input voltage, such as the micro inverter for the photovoltaic systems. Simulation results of the voltage-fed trans-quasi-Z source and the current-fed trans-quasi-Z-source inverters have verified the analysis and feature.

REFERENCES

- [1] F. Z. Peng, "Z-source inverter," *Industry Applications, IEEE Transactions on*, vol. 39, no. 2, pp. 504-510, 2003.
- [2] J. Anderson and F. Z. Peng, "Four quasi-Z-Source inverters," in *Power Electronics Specialists Conference, 2008.PESC 2008. IEEE*, 2008, pp.2743-2749.
- [3] T. Yu, X. Shaojun, Z. Chaochua, and X. Zegang, "Improved Z-Source Inverter With Reduced Z-Source Capacitor Voltage Stress and Soft-Start Capability," *Power Electronics, IEEE Transactions on*, vol. 24, no. 2, pp. 409-415, 2009.
- [4] M. Shen, A. Joseph, J. Wang, F. Z. Peng, and D. J. Adams, "Comparison of Traditional Inverters and Z-Source Inverter for Fuel Cell Vehicles," *Power Electronics, IEEE Transactions on*, vol. 22, no. 4, pp. 1453-1463, 2007.
- [5] F. Z. Peng, M. Shen, and Z. Qian, "Maximum boost control of the Z-source inverter," *Power Electronics, IEEE Transactions on*, vol. 20, no.4, pp. 833-838, 2005.
- [6] M. Shen, J. Wang, A. Joseph, F. Z. Peng, L. M. Tolbert, and D. J. Adams, "Constant boost control of the Z-source inverter to minimize current ripple and voltage stress," *Industry Applications, IEEE Transactions on*, vol. 42, no. 3, pp. 770-778, 2006.
- [7] R. Strzelecki, M. Adamowicz, N. Strzelecka, and W. Bury, "New type T-Source inverter," in *Compatibility and Power Electronics, 2009. CPE '09.*, 2009, pp. 191-195.
- [8] F. Gao, L. Poh Chiang, R. Teodorescu, and F. Blaabjerg, "Diode-Assisted Buck-Boost Voltage-Source Inverters," *Power Electronics, IEEE Transactions on*, vol. 24, no. 9, pp. 2057-2064, 2009.
- [9] C. J. Gajanayake, L. F. Lin, G. Hoay, S. P. Lam, and S. L. Kian, "Extended Boost Z-Source Inverters," *Power Electronics, IEEE Transactions on*, vol. 25, no. 10, pp. 2642-2652, Oct. 2010.
- [10] M. Zhu, K. Yu, and F. L. Luo, "Switched Inductor Z-Source Inverter," *Power Electronics, IEEE Transactions on*, vol. 25, no. 8, pp. 2150-2158, Aug 2010.
- [11] H. Xu, F. Z. Peng, L. Chen, and X. Wen, "Analysis and design of Bidirectional Z-source inverter for electrical vehicles," in *Applied Power Electronics Conference and Exposition, 2008.APEC 2008. Twenty-Third Annual IEEE*, 2008, pp. 1252-1257.
- [12] J. R. Espinoza and G. Joos, "Current-source converter on-line pattern generator switching frequency minimization," *Industrial Electronics, IEEE Transactions on*, vol. 44, no. 2, pp. 198-206, 1997.
- [13] D. N. Zmood and D. G. Holmes, "Improved voltage regulation for current-source inverters," *Industry Applications, IEEE Transactions on*, vol. 37, no. 4, pp. 1028-1036, 2001.
- [14] W. Bin, J. Pontt, J. Rodriguez, S. Bernet, and S. Kouro, "Current-Source Converter and Cycloconverter Topologies for Industrial Medium-Voltage Drives," *Industrial Electronics, IEEE Transactions on*, vol. 55, no. 7, pp. 2786-2797, 2008.
- [15] S. Yang, F. Z. Peng, Q. Lei, R. Inoshita, and Z. Qian, "Current-fed quasi-Z-source inverter with voltage buck-boost and regeneration capability," in *Energy Conversion Congress and Exposition, 2009.ECCE 2009. IEEE*, 2009, pp. 3675-3682.
- [16] P. C. Loh, D. M. Vilathgamuwa, C. J. Gajanayake, L. T. Wong, and C.P. Ang, "Z-Source Current-Type Inverters: Digital Modulation and Logic Implementation," *Power Electronics, IEEE Transactions on*, vol. 22, no. 1, pp. 169-177, 2007.
- [17] E. R. Motto, J. F. Donlon, M. Tabata, H. Takahashi, Y. Yu, and G. Majumdar, "Application characteristics of an experimental RB-IGBT (reverse blocking IGBT) module," in *Industry Applications Conference, 2004. 39th IAS Annual Meeting. Conference Record of the 2004 IEEE*, 2004, pp. 1540-1544 vol.3.
- [18] A. F. Witulski, "Introduction to modeling of transformers and coupled inductors," *Power Electronics, IEEE Transactions on*, vol. 10, no. 3, pp.349-357, 1995.
- [19] M. Shen and F. Z. Peng, "Operation Modes and Characteristics of the Z-Source Inverter With Small Inductance or Low Power Factor," *Industrial Electronics, IEEE Transactions on*, vol. 55, no. 1, pp. 89-96, 2008.
- [20] R. W. Erickson and D. Maksimovic, *Fundamentals of Power Electronics (2nd edition)*, Kluwer Academic Publishers, Norwell, MA